


ORIGINAL ARTICLE

Generation and validation of small ADAMTS13 fragments for epitope mapping of anti-ADAMTS13 autoantibodies in immune-mediated thrombotic thrombocytopenic purpura

Kadri Kangro MSc¹ | Elien Roose PhD¹ | An-Sofie Schelpe PhD¹ | Edwige Tellier PhD^{2,3} | Gilles Kaplanski MD, PhD^{2,3,4} | Jan Voorberg PhD⁵ | Simon F. De Meyer PhD¹ | Andres Männik PhD⁶ | Karen Vanhoorelbeke PhD¹ 

¹Laboratory for Thrombosis Research, IRF Life Sciences, KU Leuven Campus Kulak Kortrijk, Kortrijk, Belgium

²INSERM, INRAE, Aix-Marseille University, Marseille, France

³French Reference Center for Thrombotic Microangiopathies, France

⁴INSERM, INRAE, Hôpital de la Conception, Aix-Marseille University, Marseille, France

⁵Department of Molecular and Cellular Hemostasis, Sanquin-Academic Medical Center Landsteiner Laboratory, Amsterdam, The Netherlands

⁶Icosagen Cell Factory OÜ, Kambja vald, Tartumaa, Estonia

Correspondence

Karen Vanhoorelbeke, Laboratory for Thrombosis Research, IRF Life Sciences, KU Leuven Campus Kulak Kortrijk, Etienne Sabbelaan 53, 8500 Kortrijk, Belgium
Email: Karen.Vanhoorelbeke@kuleuven.be

Funding information

European Union's Horizon 2020 research and innovation programme under the Marie Skłodowska-Curie grant agreement, Grant/Award Number: 675746

Handling Editor: Dr Alisa Wolberg

Abstract

Background: In immune-mediated thrombotic thrombocytopenic purpura (iTTP), patients develop an immune response against the multidomain enzyme ADAMTS13. ADAMTS13 consists of a metalloprotease (M) and disintegrin-like (D) domain, 8 thrombospondin type 1 repeats (T1-T8), a cysteine-rich (C), a spacer (S), and 2 CUB domains (CUB1-2). Previous epitope mapping studies have used relatively large overlapping ADAMTS13 fragments.

Objectives: We aimed at developing small nonoverlapping ADAMTS13 fragments to fine map anti-ADAMTS13 autoantibodies in iTTP patients.

Methods: A library of 16 ADAMTS13 fragments, comprising several small (M, DT, C, S, T2-T5, T6-T8, CUB1, CUB2), and some larger fragments with overlapping domains (MDT, MDTC, DTC, CS, T2-T8, CUB1-2, MDTCS, T2-C2), were generated. All fragments, and ADAMTS13, were expressed as a fusion protein with albumin domain 1, and purified. The folding of the fragments was tested using 17 anti-ADAMTS13 monoclonal antibodies with known epitopes. An epitope mapping assay using small ADAMTS13 fragments was set up, and validated by analyzing 18 iTTP patient samples.

Results: Validation with the monoclonal antibodies demonstrated that single S and CUB1 were not correctly folded, and therefore CS and CUB1-2 fragments were selected instead of single C, S, CUB1, and CUB2 fragments. Epitope mapping of antibodies of patients with iTTP confirmed that 6 nonoverlapping ADAMTS13 fragments M, DT, CS, T2-T5, T6-T8, and CUB1-2 were sufficient to accurately determine the antibody-binding sites.

Conclusion: We have developed a tool to profile patients with iTTP according to their anti-ADAMTS13 antibodies for a better insight in their immune response.

This is an open access article under the terms of the Creative Commons Attribution-NonCommercial-NoDerivs License, which permits use and distribution in any medium, provided the original work is properly cited, the use is non-commercial and no modifications or adaptations are made.

© 2020 Research and Practice in Thrombosis and Haemostasis published by Wiley Periodicals LLC on behalf of International Society on Thrombosis and Haemostasis.

KEY WORDS

ADAMTS13 protein, antibodies, epitopes, human serum albumin, thrombotic thrombocytopenic purpura

Essentials

- Epitope fine mapping of anti-ADAMTS13 autoantibodies is lacking.
- Small nonoverlapping ADAMTS13 fragments facilitate fine mapping.
- N-terminal fusion protein ensures the secretion of the small ADAMTS13 fragments.
- A high-throughput assay for fine mapping of anti-ADAMTS13 autoantibodies was generated.

1 | INTRODUCTION

The rare life-threatening disorder immune-mediated thrombotic thrombocytopenic purpura (iTTP) is caused by autoantibodies targeting the enzyme ADAMTS13 (A Disintegrin And Metalloprotease with Thrombospondin type 1 repeats, member 13).¹ ADAMTS13 consists of a metalloprotease (M) and disintegrin-like (D) domain, 8 thrombospondin type 1 repeats (T1-T8), a cysteine-rich (C), a spacer (S), and 2 CUB domains (CUB1-2).²

The binding sites of anti-ADAMTS13 autoantibodies in patients with iTTP have been investigated for almost 2 decades.³⁻⁸ To map the anti-ADAMTS13 autoantibody immune response in patients with iTTP, different ADAMTS13 fragments covering the whole ADAMTS13 molecule expressed by different cell types have been used (Figure 1). These ADAMTS13 fragments, however, were relatively large and mainly consisted of multiple domains, like MDT, MDTCS, T2-T8, T5-CUB1-2 and CUB1-2⁵ or MD, MDTC,

MDTCS, and T2-T8⁷ fragments (Figure 1). Hence, fine mapping of anti-ADAMTS13 autoantibodies is currently lacking. Nevertheless, the epitope mapping studies using these relatively large fragments showed that the majority of the patients with iTTP have antibodies against the CS domains and that around 60% of the patients also have antibodies against other domains.^{3,5-7} However, relatively large ADAMTS13 fragments instead of the CS fragment were used in the greater part of the studies to demonstrate the presence of anti-CS antibodies.^{5,7} Indeed, small fragments like M, DT, CS, and S have been used only in small epitope mapping studies (15-25 patients with iTTP) where recombinant ADAMTS13 fragments were produced in either bacterial cells³ or insect cells⁴ (Figure 1). In larger epitope mapping studies (48-92 patients with iTTP) where ADAMTS13 fragments were expressed in mammalian cells, M, DT, CS, and S fragments were not produced. Hence, the presence of anti-CS autoantibodies was indirectly demonstrated. In addition, in these studies, the presence of anti-M and anti-DT antibodies could not be deduced

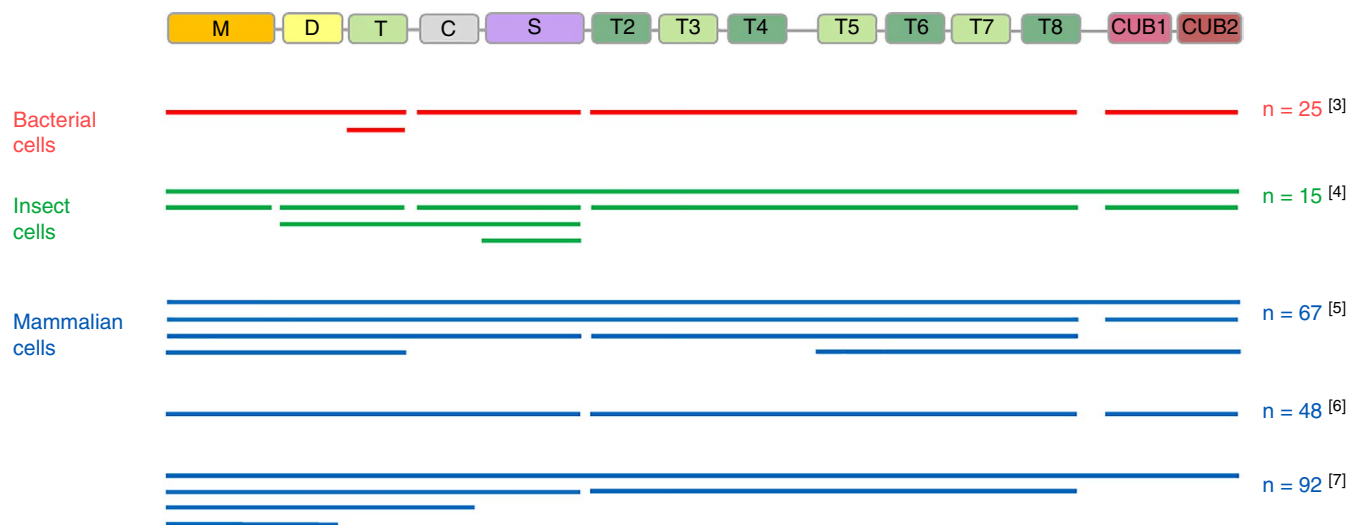


FIGURE 1 Overview of ADAMTS13 fragments used in published epitope-mapping studies of anti-ADAMTS13 autoantibodies in patients with iTTP. The different ADAMTS13 fragments used in each study are depicted by lines. The different colors refer to the type of cells used in each study; red: bacterial cells, green: insect cells, blue: mammalian cells. The number of patients analyzed (n) in each study is depicted. Only epitope-mapping studies performed on cohorts of 15 patients or more with iTTP are represented. M: metalloprotease domain; D: disintegrin-like domain; T: thrombospondin type 1 repeats (T1-T8); C: cysteine-rich domain; S: spacer domain; CUB1 and CUB2: complement component C1r/C1s, epidermal growth factor-related sea urchin protein (Uegf) and bone morphogenetic protein 1

(Figure 1). Although the CUB1-2 domains were expressed in mammalian cells for direct identification of anti-ADAMTS13 autoantibodies in 2 studies^{5,6}, in another study⁷ the presence of anti-CUB1-2 autoantibodies was indirectly demonstrated (Figure 1). Finally, other small ADAMTS13 fragments like T2-T5 and T6-T8, or even smaller fragments were never used in epitope mapping studies. The lack of using mammalian expressed small ADAMTS13 fragments for epitope mapping might be related to the difficulties of expressing small, naturally nonsecretory fragments in mammalian cells.⁹

Fine-mapping of anti-ADAMTS13 autoantibodies is needed as this will lead to a more detailed insight into the immune response in iTTP patients. This detailed insight is a prerequisite to better understand how anti-ADAMTS13 autoantibodies clear¹⁰ and/or inhibit¹¹ ADAMTS13 and which ADAMTS13 domains are targeted by these autoantibodies. In addition, as we recently demonstrated that anti-ADAMTS13 autoantibodies also induce an open ADAMTS13 conformation in iTTP,¹² a detailed epitope mapping will help to understand which ADAMTS13 domains are targeted by these anti-ADAMTS13 autoantibodies that open ADAMTS13.

In this study, we aimed at generating an ADAMTS13 domain library consisting of relatively small nonoverlapping ADAMTS13 fragments. To realize high-level expression of ADAMTS13 and its fragments, we used the QMCF technology¹³ and expressed ADAMTS13 and its fragments as fusion proteins with the albumin domain 1 (AD1) of human serum albumin.¹⁴ Fusion proteins are used to enhance protein expression and secretion of small fragments of a protein that are not readily produced or secreted from cells.⁹

Finally, we developed and validated an epitope mapping enzyme-linked immunosorbent assay (ELISA) based on coated ADAMTS13 and its fragments using 18 iTTP plasma samples. High-level expression of ADAMTS13 and its fragments, as well as the availability of an epitope-mapping ELISA, will allow high-throughput epitope mapping of anti-ADAMTS13 autoantibodies in large cohorts of patients with iTTP ($n > 100$) in the future.

2 | MATERIALS AND METHODS

2.1 | Monoclonal anti-ADAMTS13 antibodies

The 14 murine monoclonal anti-ADAMTS13 antibodies used in this study were developed in-house using standard immunization strategies, and their epitopes have been identified previously (Figure S1). Antibodies 3H9,^{15,16} 6A6,¹⁶ and 16A12¹⁷ are directed against the M domain of ADAMTS13; 4G12¹⁷ against T1; 1C9¹⁷ against the TC fragment; 1C4¹⁸, 3E4¹⁷, 7D5¹⁷, and 15D1¹⁷ against the S domain; 4B9¹⁶ against the T4-T5 fragment; 19H4¹⁶ against the T8 fragment; 12H6^{16,19} and 17G2¹⁶ against CUB1; and 7H12¹⁶ against CUB2. The 3 human monoclonal anti-ADAMTS13 antibodies used in this study were cloned from B cells from patients with iTTP, and their epitopes have been identified previously: I-9²⁰ and II-1²¹ are against the S domain, and ELH2-1²² is against the T2-T3 fragment (Figure S1)

2.2 | Patient samples

In this study, the plasma of 18 patients with iTTP from Aix-Marseille University were investigated. The same 18 iTTP plasma samples were previously used to determine the ADAMTS13 conformation.¹² Briefly, written informed consent in accordance with the Declaration of Helsinki was taken from each patient, and the study protocol was approved by the Ethics Committee of Projet National de Recherche Clinique 2007 (N° #2007/23; Marseille, France). Citrated plasma samples were taken during the acute phase, when ADAMTS13 activity was $<10\%$.¹² All patients had positive (>15 IU/mL) anti-ADAMTS13 antibody titers,¹² previously measured with the Technozym ADAMTS-13 INH ELISA kit (Technoclone, Vienna, Austria).

2.3 | Cloning of the ADAMTS13 fragments

A large library consisting of full-length ADAMTS13 and 16 ADAMTS13 fragments was generated (Figure 2A). The mammalian expression vector pQMCF¹³ containing albumin domain 1 (pQMCF-AD1) was modified by adding 2 restriction sites (of the enzymes *NheI* and *KpnI*), following a V5 tag, and a hexahistidine tag (H6) to create pQMCF-AD1-V5-H6. Fourteen fragments of ADAMTS13 were generated by polymerase chain reaction (PCR) amplification using primers (Table S1) to introduce the restriction sites mentioned above to the PCR products for cloning. The PCR products were then digested with FastDigest *NheI* and *KpnI* enzymes (ThermoFisher Scientific, Waltham, MA, USA), and inserted into the *NheI* and *KpnI* digested pQMCF-AD1-V5-H6 expression vector by T4 DNA Ligase (ThermoFisher Scientific). Expression vectors containing MDTCS, T2-C2, or ADAMTS13 were cloned using ≥ 1 sequential cloning steps. A more detailed description of the generation of the expression vectors can be found in Supplementary Materials and Methods.

2.4 | Production of ADAMTS13 fragments

All pQMCF-AD1-V5-H6 vectors containing the AD1-ADAMTS13 fragments, and the single AD1 fragment (Figure 2A) were transiently transfected into the Chinese hamster ovary (CHO)-derived cell line CHOEBNALT85 from QMCF technology¹³ using the chemical transfection reagent Reagent 007 (Icosagen Cell Factory, Kambja, Estonia) according to the manufacturer's instructions.²³ CHOEBNALT85 is specifically designed for prolonged production of proteins in association with the pQMCF vectors. For pilot production, transfected cells were grown in 70 mL of serum-free BalanCD Transfectory CHO media (Irvine Scientific, Santa Ana, CA, USA) supplemented with 6 mmol/L of Gibco GlutaMAX Supplement (Life Technologies, Rockville, MD, USA) and 1% penicillin-streptomycin (Life Technologies) on

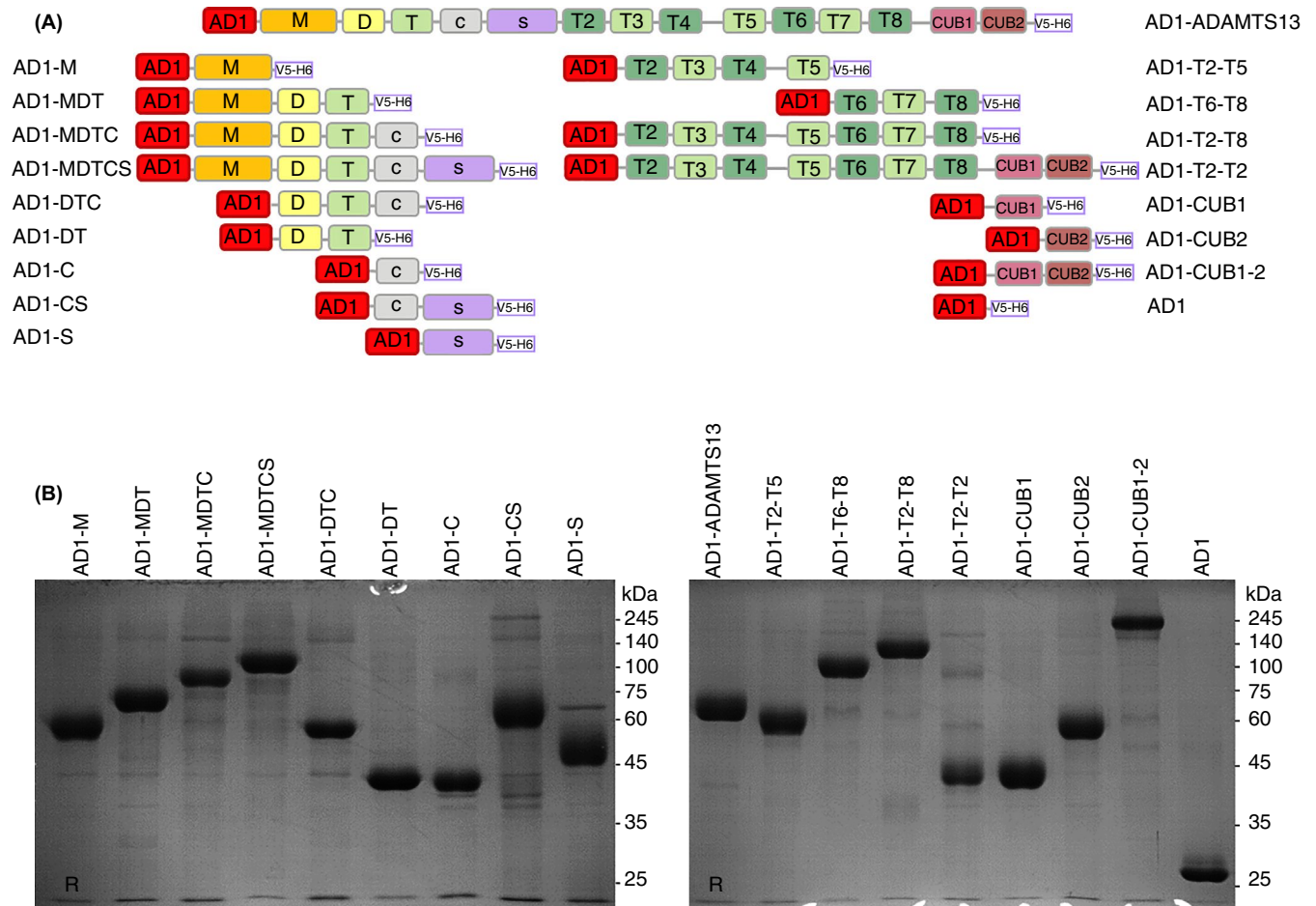


FIGURE 2 The large library of ADAMTS13 fragments generated in this study. (A) Schematic representation of full-length ADAMTS13 and 16 ADAMTS13 fragments consisting of a single domain or multiple domains of ADAMTS13: M, MDT, MDTC, DTC, DT, C, CS, S, T2-T5, T6-T8, T2-T8, CUB1, CUB2, CUB1-2, MDTCS, and T2-C2. All fragments have an N-terminal albumin domain 1 (AD1) and a C-terminal V5 and H6 tag. CHOEBNALT85 cells were transiently transfected with plasmids expressing AD1-M, AD1-MDT, AD1-MDTC, AD1-MDTCs, AD1-DTC, AD1-DT, AD1-C, AD1-CS, AD1-S, AD1-T2-T5, AD1-T6-T8, AD1-T2-T8, AD1-T2-C2, AD1-CUB1, AD1-CUB2, AD1-CUB1-2, AD1-ADAMTS13, and AD1. (B) Recombinant proteins were purified using affinity chromatography, and analyzed using SDS-PAGE (2 μ g loaded) under reducing (R) conditions. The gel was stained using Coomassie Brilliant blue

an orbital shaker platform at 37°C in the presence of 8% CO₂. Three days after transfection, the temperature was shifted to 30°C to cause a growth arrest mainly in the G1 phase of the cell cycle, thereby increasing the specific productivity.²⁴ Feeding with Feed 4 (10%, Irvine Scientific) at regular intervals of 3, 6, and 8 days after transfection was added to prolong culture viability and productivity.²⁵ For the production in large volumes up to 360 mL, the cells were grown in serum-free CHO TF media (Xell, Bielefeld, Germany) supplemented with 6 mmol/L Gibco GlutaMAX Supplement (Life Technologies), and 1% penicillin-streptomycin (Life Technologies), and feeding was performed as described above with Basic Feed (10%, Xell). The culture media was harvested 10 days after transfection (1000 g, 15°C, 30 min), and stored at -20°C in the presence of 0.5 mmol/L serine protease inhibitor phenylmethylsulfonyl fluoride, until purification.

2.5 | Purification of ADAMTS13 fragments from culture media

The fragments were purified using immobilized metal ion affinity chromatography. The culture media were filtered (0.45 μ m) and loaded overnight in the presence of 0.01% sodium azide (NaN₃, Carl Roth GmbH + Co. KG, Karlsruhe, Germany) onto a prepacked 1 mL HisTrap excel column containing nickel (Ni Sepharose excel) affinity resin (GE Healthcare, Princeton, NJ, USA). The column was washed with 30 mL of 350 mmol/L NaCl and 17.5 mmol/L imidazole in phosphate buffered saline (PBS), and eluted with 350 mmol/L NaCl and 500 mmol/L imidazole in PBS. The buffer of purified protein was exchanged into Dulbecco's PBS buffer (Pan-Biotech, Aidenbach, Germany), via gel filtration using 3 columns of 5-mL HiTrap Desalting columns with prepacked Sephadex G-25 resin (GE Healthcare).

The purified proteins (2 µg loaded) were analyzed using sodium dodecyl sulfate–polyacrylamide gel electrophoresis (SDS-PAGE) followed by Coomassie Brilliant blue G-250 (AppliChem, Darmstadt, Germany) staining under reducing (20 mmol/L dithiothreitol) conditions. The concentration of purified protein was determined using a NanoDrop 2000c Spectrophotometer (ThermoFisher Scientific).

2.6 | Binding of monoclonal anti-ADAMTS13 antibodies to generated AD1-ADAMTS13 fragments

The wells of Nunc MaxiSorp flat-bottom 96-well plates (ThermoFisher Scientific) were coated with the purified AD1-ADAMTS13 fragments at 5 µg/mL in PBS overnight at 4°C. This was followed by blocking with a PBS solution containing 2% bovine serum albumin (BSA; PAN-Biotech), 0.05% Tween 20 (Carl Roth GmbH + Co. KG), 0.1% ProClin 150 (Sigma-Aldrich, St Louis, MO, USA) for 2 hours at room temperature (RT). A 1-in-2 dilution series of murine anti-M (3H9, 6A6, 16A12) antibodies were added to coated AD1-ADAMTS13, AD1-MDTCS, AD1-M, AD1-MDT, AD1-MDTC, AD1-DTC, AD1-DT, AD1-CS, and to coated AD1-T2-C2 and AD1 as negative controls, with a start concentration of 1 µg/mL. Similarly, murine anti-DT (4G12), murine anti-TC (1C9), murine or human anti-S (1C4, 3E4, 7D5, 15D1, I-9, II-1) antibodies were added to coated AD1-ADAMTS13, AD1-MDTCS, AD1-MDT, AD1-MDTC, AD1-DTC, AD1-DT, AD1-C, AD1-CS, AD1-S, and to coated AD1-T2-C2 and AD1 as negative controls. Human anti-T2-T3 (ELH2-1), murine anti-T4-T5 (4B9), murine anti-T8 (19H4), murine anti-CUB1 (12H6, 17G2) and murine anti-CUB2 (7H12) antibodies were added to coated AD1-ADAMTS13, AD1-T2-C2, AD1-T2-T5, AD1-T6-T8, AD1-T2-T8, AD1-CUB1, AD1-CUB2, AD1-CUB1-2, and to coated AD1-MDTCS and AD1 as negative controls, in a 1-in-2 dilution series with a start concentration of 1 µg/mL (except antibody ELH2-1, which was added at a start concentration of 16 µg/mL). On each 96-well plate murine anti-M monoclonal antibody 3H9, or human anti-S monoclonal antibody II-1 was added in a 1-in-2 dilution series (start concentration 1 µg/mL) to coated AD1-ADAMTS13 as a reference for the binding of murine or human anti-ADAMTS13 monoclonal antibodies, respectively. The monoclonal antibodies were diluted in dilution buffer (1% BSA, 0.05% Tween 20, 0.1% ProClin 150 in PBS) and incubated for 1 hour at 37°C. The bound mouse or human antibodies were detected by adding horseradish peroxidase (HRP)-labeled goat anti-Mouse IgG H&L (1/10 000; Abcam, Cambridge, England), or anti-human IgG (Fc specific)-peroxidase antibody produced in goat (1/10 000; Sigma-Aldrich), respectively, in dilution buffer for 1 hour at RT. Colorimetric development was performed by using 3,3',5,5'-tetramethylbenzidine VII substrate (Biopanda Diagnostics). The reaction was stopped using 0.5 mol/L H₂SO₄, and absorbance was measured at 450 nm. The optical density (OD) value corresponding to the binding of 3H9 or II-1 at 0.0156 µg/mL to AD1-ADAMTS13 was set as 1 to calculate the relative OD values.

2.7 | Epitope mapping of anti-ADAMTS13 autoantibodies in plasma samples of patients with iTTP

The wells of Nunc MaxiSorp flat-bottom 96-well plates were coated with the purified fragments of AD1-ADAMTS13, AD1-MDTCS, AD1-T2-C2, AD1-M, AD1-DT, AD1-CS, AD1-T2-T5, AD1-T6-T8, AD1-CUB1-2, or AD1 at 5 µg/mL in PBS overnight at 4°C, and blocked as described above. The patient plasma samples were added in a 1-in-40 dilution in the dilution buffer and incubated for 1 hour at 37°C. Bound antibodies were detected by the anti-human IgG (Fc specific)-peroxidase antibody produced in goat (1/10 000; Sigma-Aldrich), followed by coloring development as described above. The relative OD values were calculated as described above using antibody II-1. Next, the relative OD values obtained after binding of patient anti-ADAMTS13 autoantibodies to AD1-ADAMTS13, AD1-MDTCS, AD1-T2-C2, AD1-M, AD1-DT, AD1-CS, AD1-T2-T5, AD1-T6-T8, or AD1-CUB1-2 were compared to the relative OD obtained after binding to AD1. For example, if the patient plasma contained anti-MDTCS autoantibodies, then the relative OD of binding of the antibodies to AD1-MDTCS was significantly different from the relative OD of binding to AD1. As an alternative method to determine positive antibody titers, the mean relative OD + 3× standard deviation (SD) of the AD1 sample was used as a cutoff for positivity. A residual value >0.2 after subtraction of the cutoff value was considered to indicate a positive antibody titer.

2.8 | Statistical analysis

The data were analyzed using 1-way analysis of variance (ANOVA) followed by Dunnett's multiple comparisons post hoc test in Prism version 8.0.1 (GraphPad Software, La Jolla, CA, USA).

3 | RESULTS

3.1 | All generated ADAMTS13 fragments are expressed well

We generated a large library of 16 ADAMTS13 fragments, namely M, MDT, MDTC, DTC, DT, C, CS, S, T2-T5, T6-T8, T2-T8, CUB1, CUB2, CUB1-2, MDTCS, T2-C2, and full-length ADAMTS13 (Figure 2A). Fragments M, DT, C, S, T2-T5, T6-T8, CUB1, and CUB2 were nonoverlapping fragments that cover the entire ADAMTS13 sequence, and are in theory sufficient to perform the epitope mapping. Fragments MDT, MDTC, DTC, CS, T2-T8, and CUB1-2 were included as alternative supportive fragments for circumstances where the individual domains M, C, S, CUB1, and CUB2 or small fragments like T2-T5 and T6-T8 would not be well expressed. All 16 fragments and full-length ADAMTS13 were generated and expressed as fusion proteins to AD1 (Figure 2A). AD1 was added as an N-terminal fusion partner to increase the secretion of all fragments.⁹ The single AD1 domain was

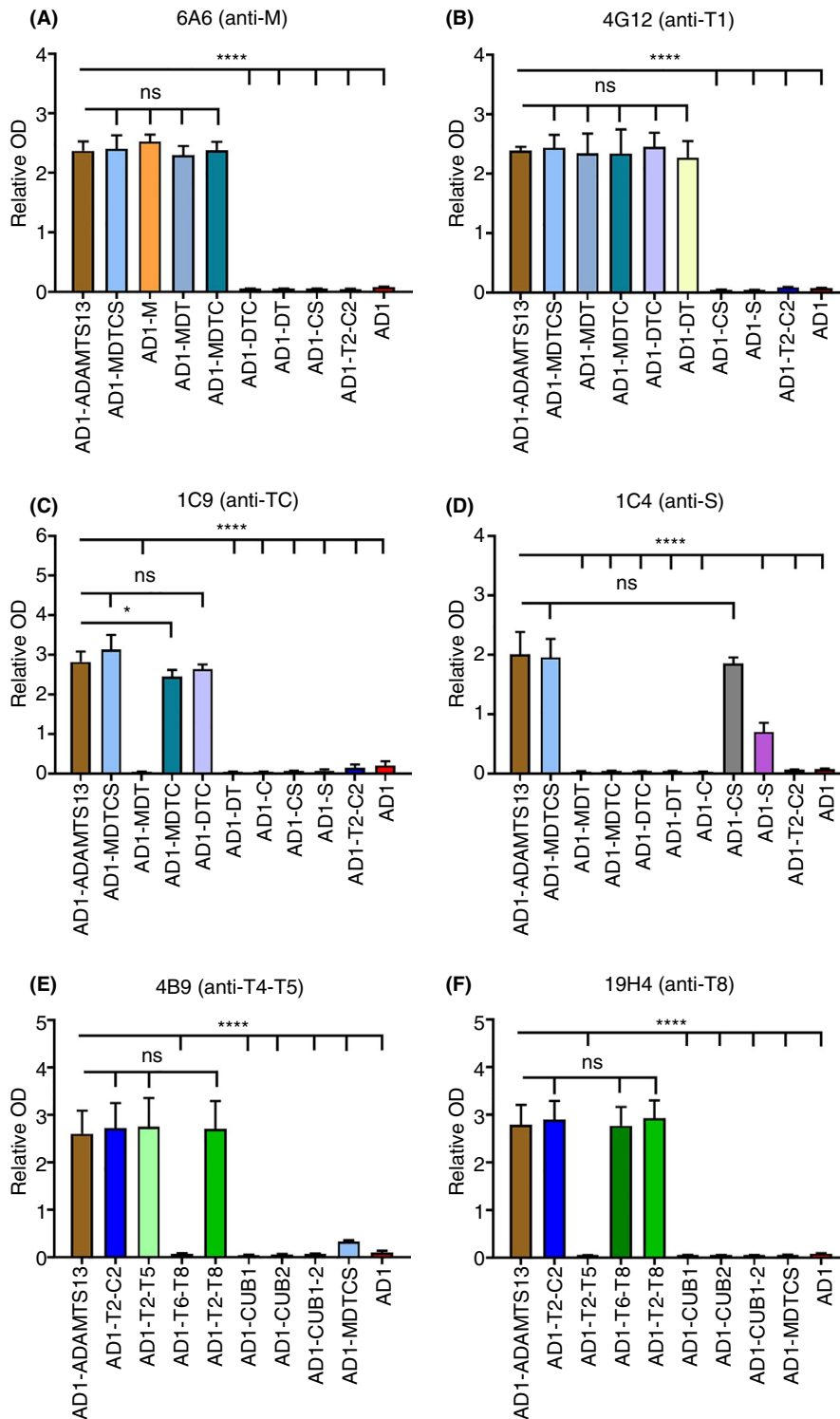


FIGURE 3 Binding of anti-ADAMTS13 monoclonal antibodies to AD1-ADAMTS13 fragments. Binding of murine monoclonal antibodies (A) 6A6 (anti-M), (B) 4G12 (anti-T1), (C) 1C9 (anti-TC), (D) 1C4 (anti-S), (E) 4B9 (anti-T4-T5), (F) 19H4 (anti-T8), (G) 17G2 (anti-CUB1), (H) 7H12 (anti-CUB2) to the coated AD1-ADAMTS13 fragments (AD1-M, AD1-MDT, AD1-MDTC, AD1-MDTCS, AD1-DTC, AD1-DT, AD1-C, AD1-CS, AD1-S, AD1-T2-T5, AD1-T6-T8, AD1-T2-T8, AD1-T2-C2, AD1-CUB1, AD1-CUB2, AD1-CUB1-2, or full-length AD1-ADAMTS13) and AD1. Bound antibodies were detected using horseradish peroxidase-labeled goat-anti-mouse antibody. Relative optical density (OD) values are represented as mean \pm SD ($n = 3$). The binding of each antibody to AD1-ADAMTS13 fragment was compared to the binding to AD1-ADAMTS13, * $P < .05$; **** $P < .0001$; ns: not significant, 1-way analysis of variance, post-hoc Dunnett's multiple comparisons test

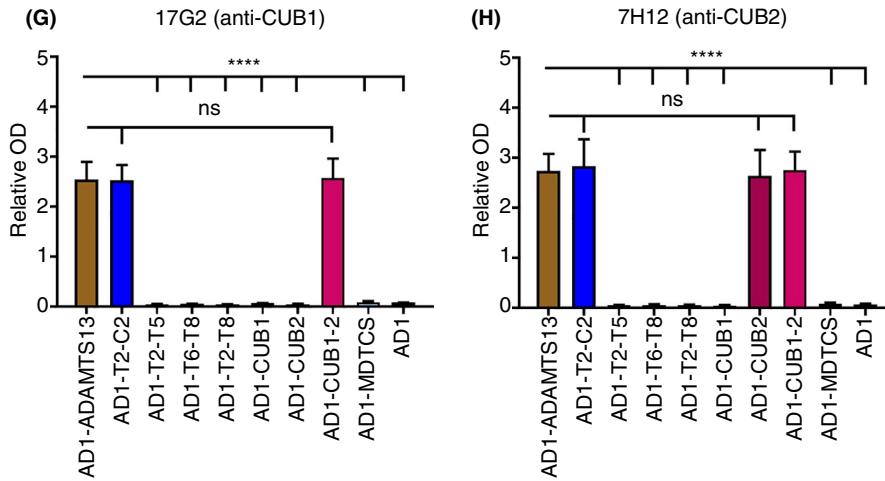


FIGURE 3 Continued

expressed to be used as a negative control in the epitope-mapping assay (Figure 2A).

AD1-ADAMTS13 and all AD1-ADAMTS13 fragments were efficiently secreted in the culture medium at a concentration up to 100 $\mu\text{g}/\text{mL}$ (data not shown), and were purified from their culture media using affinity chromatography. The obtained yield of the recombinant proteins after purification was high and was on average 7 mg per transient transfection (data not shown). Most of the recombinant proteins migrated at a distance (Figure 2B) that is in agreement with their calculated molecular weight (Table S1), except for fragments like AD1-S, AD1-CS, AD1-MDTCS, and AD1-ADAMTS13 (Figure 2B), which migrated at a higher molecular weight compared to the calculated molecular weight. This might be probably due to glycosylation^{26,27} as recombinant ADAMTS13, which has the calculated molecular weight of 145 kDa, has been shown to be highly glycosylated.²⁸⁻³⁰

3.2 | General folding of the ADAMTS13 fragments

The general folding of the ADAMTS13 domains in the AD1-ADAMTS13 fragments was compared to the folding of the domains in AD1-ADAMTS13 using 14 murine and 3 human anti-human ADAMTS13 monoclonal antibodies known to target epitopes in specific domains of ADAMTS13 (Figure S1).

The conformation of the M domain was comparable in all constructs carrying an M domain. Indeed, AD1-ADAMTS13, AD1-MDTCS, AD1-M, AD1-MDT, and AD1-MDTC were well recognized by anti-M monoclonal antibodies 6A6 (Figure 3A), 3H9, and 16A12 (Figure S2A-B). Binding of the anti-T1 monoclonal antibody 4G12 showed that the epitopes were available in fragment AD1-DT, as well as AD1-ADAMTS13, AD1-MDTCS, AD1-MDT, AD1-MDTC, and AD1-DTC (Figure 3B). The epitope of the anti-TC monoclonal antibody 1C9 was equally accessible in AD1-ADAMTS13, AD1-MDTCS, and AD1-DTC (Figure 3C), although there was a slight difference in binding to AD1-MDTC compared to AD1-ADAMTS13.

The epitopes of anti-S antibodies 1C4 (Figure 3D), 3E4, 7D5, 15D1, I-9, II-1 (Figure S2C-G) were equally accessible in AD1-ADAMTS13, AD1-MDTCS and AD1-CS fragments. However, the binding to AD1-S fragment was significantly reduced ($P < .001$) for antibodies 1C4 (Figure 3D), 3E4, 7D5, 15D1, and I-9 (Figure S2C-F), as well as for antibody II-1 ($P < .05$; Figure S2G). This suggests that the epitopes in the AD1-S fragment might not be accessible for several anti-S antibodies most likely due to an aberrant folding of the single S domain.

The epitope of the anti-T4-T5 antibody 4B9 (Figure 3E) was accessible in all fragments containing T2-T5, namely in AD1-ADAMTS13, AD1-T2-C2, AD1-T2-T5 and AD1-T2-T8. The epitope of the anti-T2-T3 antibody ELH2-1 was equally accessible in AD1-ADAMTS13, AD1-T2-C2, and AD1-T2-T8, while the binding to the AD1-T2-T5 fragment was decreased (Figure S2H). The anti-T8 antibody 19H4 equally well recognized AD1-ADAMTS13, AD1-T2-C2, AD1-T6-T8, and AD1-T2-T8 (Figure 3F).

Using anti-CUB1 antibodies 17G2 (Figure 3G) and 12H6 (Figure S2I) showed that their epitopes were accessible in AD1-ADAMTS13, AD1-T2-C2 and AD1-CUB1-2 constructs. However, antibodies 17G2 and 12H6 did not bind to the CUB1 domain in the AD1-CUB1 fragment (Figure 3G; Figure S2I), indicating that the folding of the CUB1 domain in this construct is compromised. In contrast, anti-CUB2 antibody 7H12 (Figure 3H) did recognize the individual CUB2 domain in the AD1-CUB2 fragment and in all other fragments containing CUB2, which are AD1-ADAMTS13, AD1-T2-C2, and AD1-CUB1-2.

Validation with the 17 monoclonal antibodies showed that for AD1-M, AD1-MDT, AD1-MDTC, AD1-MDTCS, AD1-DTC, AD1-DT, AD1-CS, AD1-T2-T5, AD1-T6-T8, AD1-T2-T8, AD1-T2-C2, AD1-CUB2, AD1-CUB1-2, and AD1-ADAMTS13 the epitopes are well accessible and hence these data suggest that the folding of these domains is not compromised. However, these data also suggest that the folding of the fragments AD1-S and AD1-CUB1 is compromised, since several monoclonal antibodies showed either reduced binding (1C4, 3E4, 7D5, 15D1, I-9, II-1), or no binding at all (17G1, 12H6) to

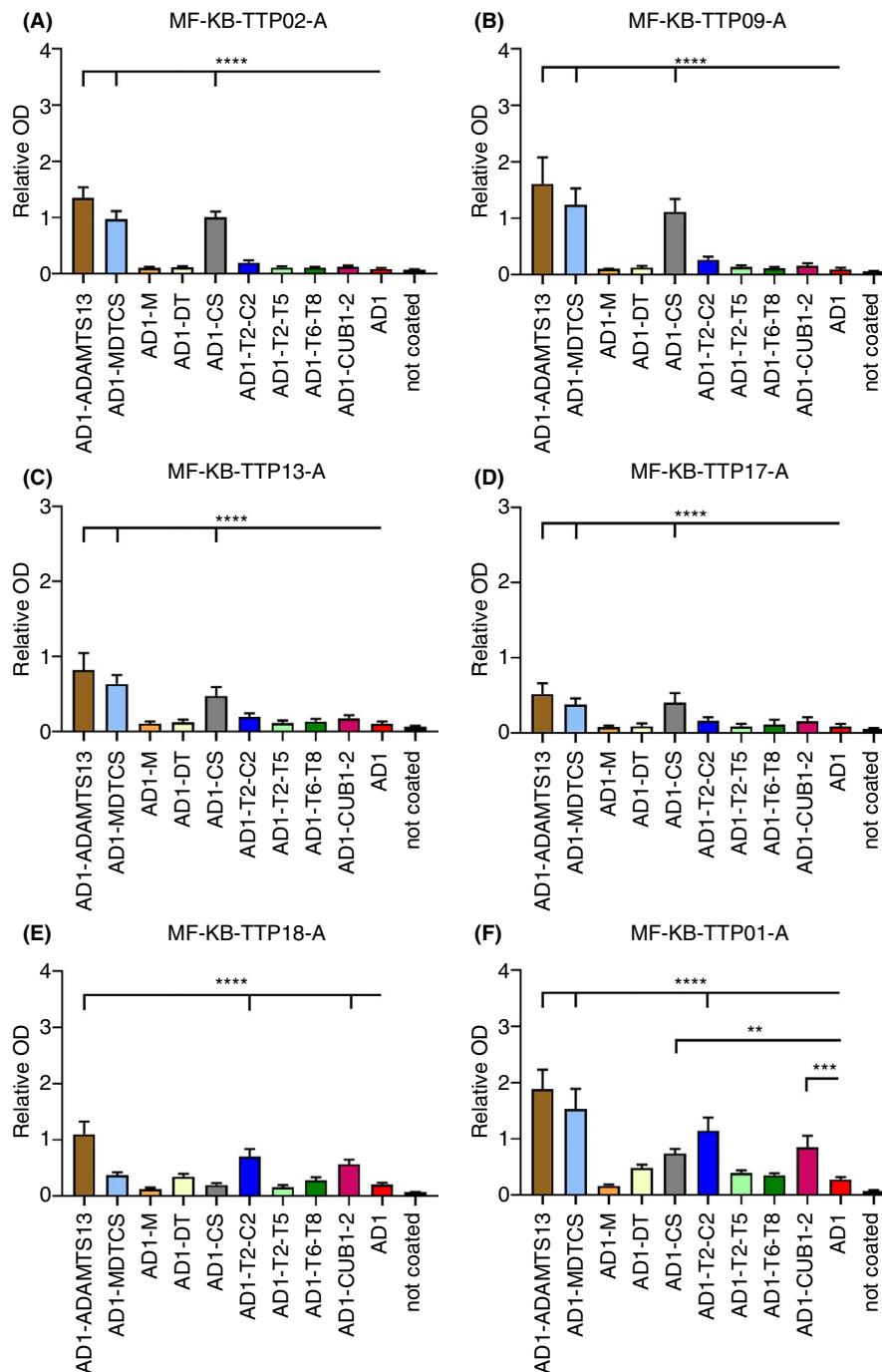


FIGURE 4 Epitope fine mapping of anti-ADAMTS13 autoantibodies in the plasma of patients with immune-mediated thrombotic thrombocytopenic purpura (iTTP). (A-R) Plasma of patients with iTTP was added to the coated albumin domain 1 (AD1)-ADAMTS13 fragments (AD1-M, AD1-DT, AD1-CS, AD1-T2-T5, AD1-T6-T8, AD1-CUB1-2, AD1-MDTCS, AD1-T2-C2, or full-length AD1-ADAMTS13) and AD1. Bound antibodies were detected using horseradish peroxidase-labeled goat-anti-human (Fc specific) antibody. Relative OD values are represented as mean \pm SD ($n = 3$). The binding of antibodies from each patient to AD1 fragment was compared to the binding to each AD1-ADAMTS13 fragment, * $P < .05$; ** $P < .01$; *** $P < .001$; **** $P < .0001$, 1-way analysis of variance, post hoc Dunnett's multiple comparisons test. (S) The epitopes of the anti-ADAMTS13 autoantibodies from the 18 patients with iTTP are represented in a heatmap using the ADAMTS13 fragments as described above. Positive antibody titers are marked in green, and no detectable antibodies are marked in red. Samples with too low anti-ADAMTS13 antibody titers in which it was not possible to determine the full antibody profile are shown in gray

these fragments. Therefore, AD1-S and AD1-CUB1 could not be used for the epitope mapping of anti-ADAMTS13 autoantibodies. Since we did not have an anti-C monoclonal antibody, we could not determine whether the C domain was well folded or not. Based on

these data, we selected the following nonoverlapping ADAMTS13 fragments, AD1-M, AD1-DT, AD1-CS, AD1-T2-T5, AD1-T6-T8, and AD1-CUB1-2, to perform a full epitope mapping of anti-ADAMTS13 autoantibodies in patients with iTTP.

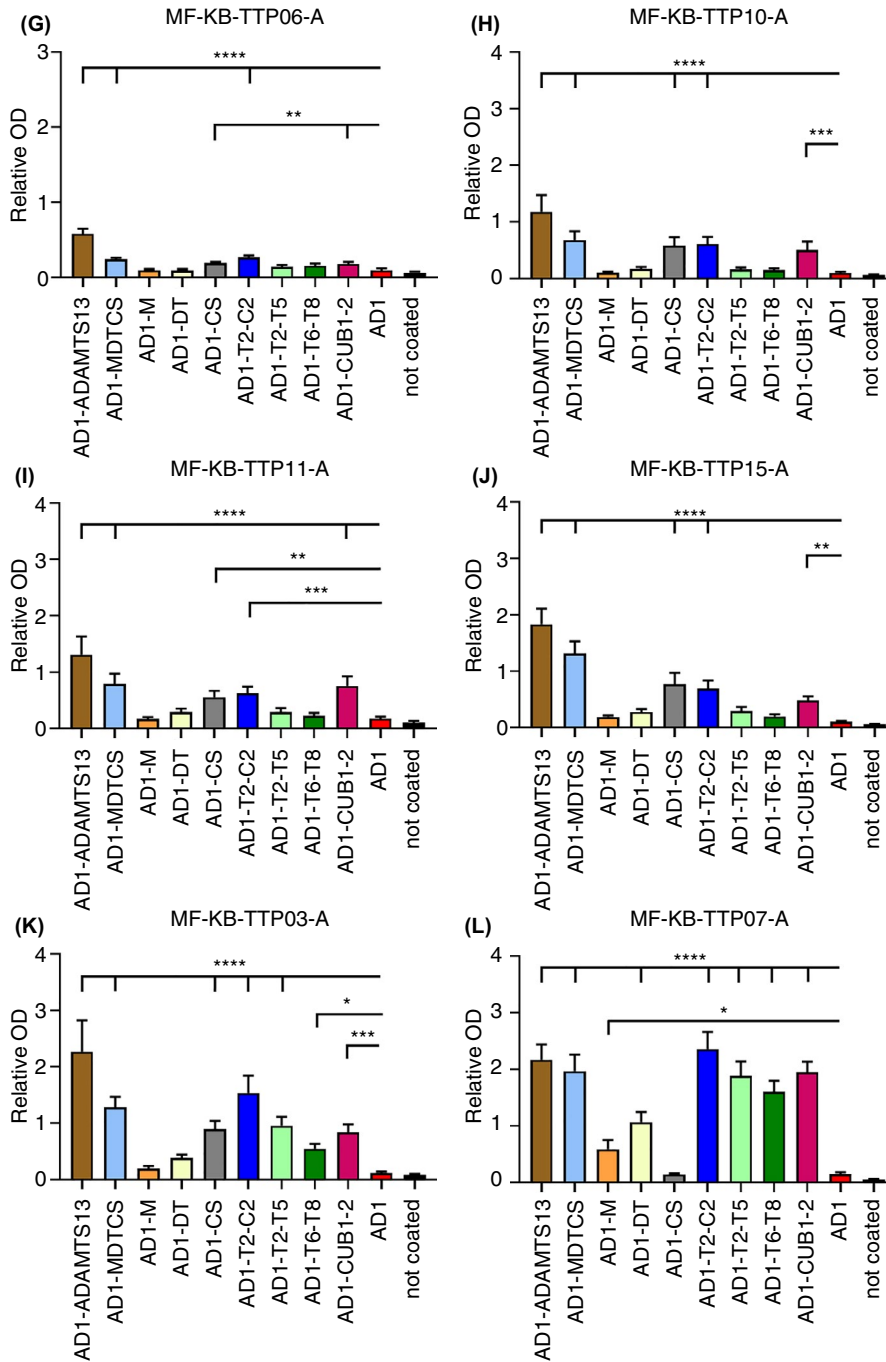


FIGURE 4 Continued

3.3 | Epitope mapping of antibodies from plasma of patients with iTTP using the selected ADAMTS13 fragments

Next, we generated an epitope-mapping ELISA and used acute-phase plasma samples of 18 patients with iTTP to validate this ELISA. As discussed above, only working with the nonoverlapping ADAMTS13 fragments, AD1-M, AD1-DT, AD1-CS, AD1-T2-T5, AD1-T6-T8, and AD1-CUB1-2 (Figure 2A), is sufficient to obtain the full epitope mapping of the anti-ADAMTS13 autoantibodies in these

patients. As internal controls, we also used AD1-ADAMTS13, AD1-MDTCS, AD1-T2-C2, and AD1 (Figure 2A).

Therefore, the epitope mapping with 6 small fragments, and with 3 large fragments for internal control, and AD1 fragment, was done in triplicate for all 18 iTTP patients (Figure 4A-R). The internal control AD1-ADAMTS13 showed that all 18 plasma samples contained anti-ADAMTS13 autoantibodies as expected (Figure 4), since the relative OD of binding to AD1-ADAMTS13 was significantly higher than the relative OD of binding to AD1. In addition, 5 patients had only detectable anti-MDTCS antibodies (Figure 4A-D, Q), 1 patient

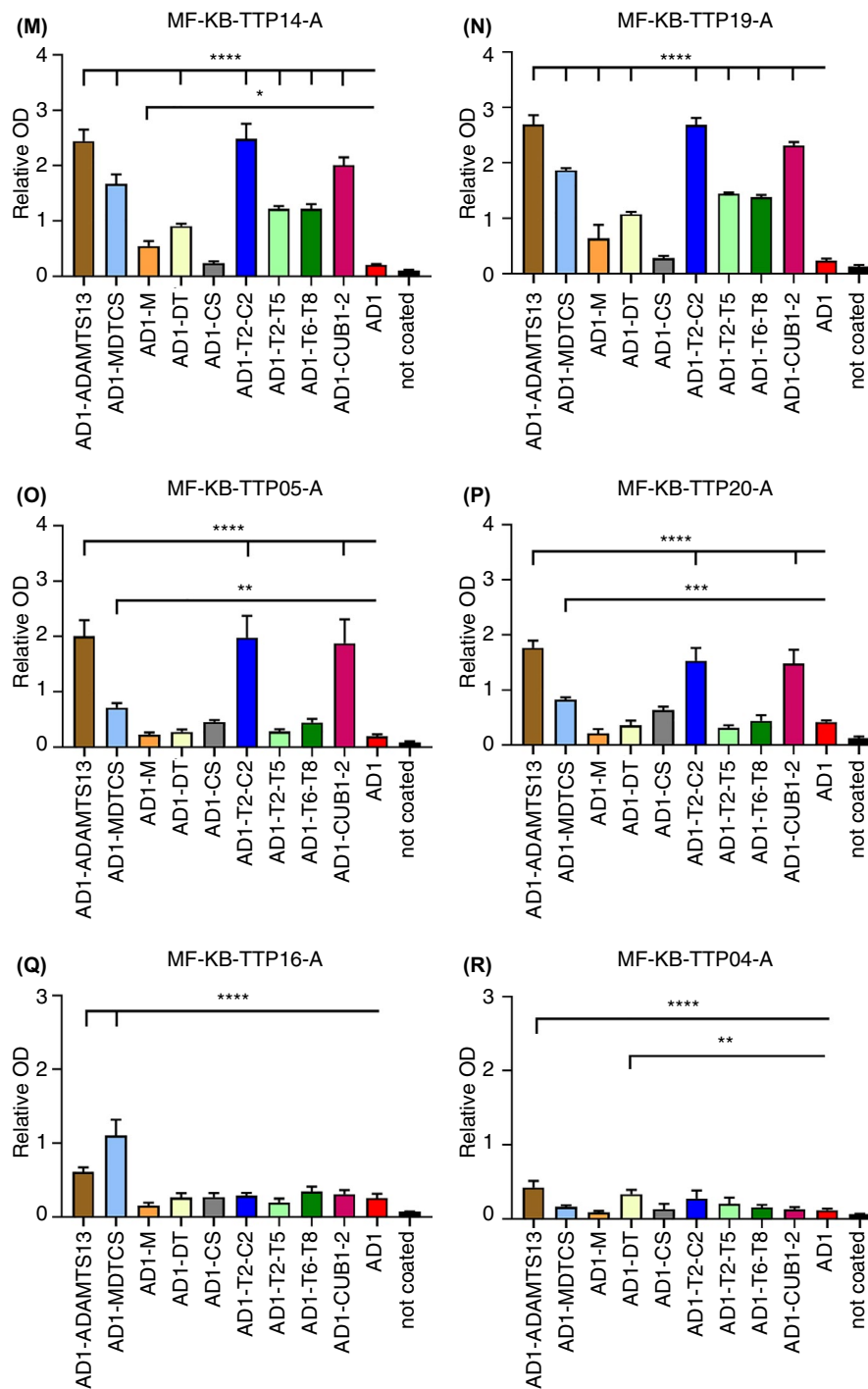


FIGURE 4 Continued

had only detectable anti-T2-C2 antibodies (Figure 4E), and 11 had both anti-MDTCS and anti-T2-C2 antibodies (Figure 4F-P). In one patient, anti-MDTCS or anti-T2-C2 antibodies could not be detected (Figure 4R). From the 5 patients with only detectable anti-MDTCS antibodies, 4 had only detectable anti-CS antibodies (Figure 4A-D). The only patient with detectable anti-T2-C2 antibodies, had only detectable anti-CUB1-2 antibodies (Figure 4E). From the patients with both anti-MDTCS and anti-T2-C2 antibodies, 5 patients had anti-CS and anti-CUB1-2 antibodies (Figure 4F-J), and 1 patient had anti-CS,

anti-T2-T5, anti-T6-T8, and anti-CUB1-2 antibodies (Figure 4K). The most polyclonal antibody response was seen in 3 patient samples (Figure 4L-N) which had anti-M, anti-DT, anti-T2-T5, anti-T6-T8, and anti-CUB1-2 antibodies. In patients MF-KB-TTP05-A (Figure 4O) and MF-KB-TTP20-A (Figure 4P), although anti-T2-C2 antibodies could be further fine mapped, a more detailed anti-MDTCS antibody profile could not be determined because the anti-MDTCS antibody titer was too low. As expected, samples MF-KB-TTP16-A (Figure 4Q) and MF-KB-TTP04-A (Figure 4R) with very low anti-ADAMTS13

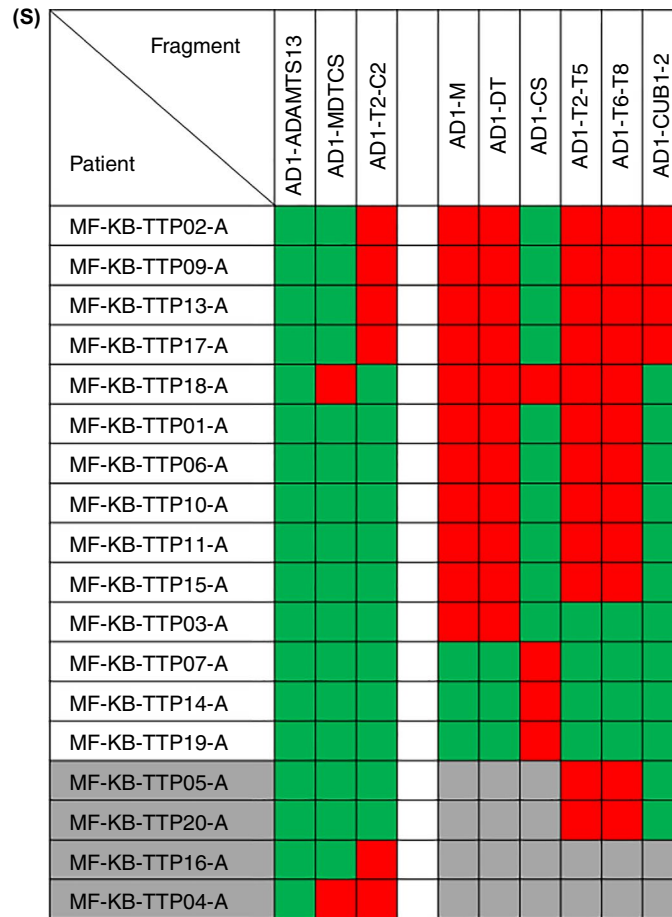


FIGURE 4 Continued

antibody titers could not be further fine mapped. The fine-mapping results are summarized in Figure 4S, which gives an overview of the antibody binding sites, and enables to determine the antibody profiles for iTTP patients. **FIGURE 4** Epitope fine mapping of anti-ADAMTS13 autoantibodies in the plasma of patients with immune-mediated thrombotic thrombocytopenic purpura (iTTP). (A-R) Plasma of patients with iTTP was added to the coated albumin domain 1 (AD1)-ADAMTS13 fragments (AD1-M, AD1-DT, AD1-CS, AD1-T2-T5, AD1-T6-T8, AD1-CUB1-2, AD1-MDTCS, AD1-T2-C2, or full-length AD1-ADAMTS13) and AD1. Bound antibodies were detected using horseradish peroxidase-labeled goat-anti-human (Fc specific) antibody. Relative OD values are represented as mean \pm SD ($n = 3$). The binding of antibodies from each patient to AD1 fragment was compared to the binding to each AD1-ADAMTS13 fragment, $*P < .05$; $**P < .01$; $***P < .001$; $****P < .0001$, 1-way analysis of variance, post hoc Dunnett's multiple comparisons test. (S) The epitopes of the anti-ADAMTS13 autoantibodies from the 18 patients with iTTP are represented in a heatmap using the ADAMTS13 fragments as described above. Positive antibody titers are marked in green, and no detectable antibodies are marked in red. Samples with too low anti-ADAMTS13 antibody titers in which it was not possible to determine the full antibody profile are shown in gray

When studying large cohorts (>100) of iTTP plasma samples, performing triplicate experiments of each plasma sample is not

straightforward, nor every time possible due to the limited volume of available plasma. Therefore, we reanalyzed the data and determined the mean relative OD of AD1 + 3x SD as a cutoff for positivity (as without 3 repeats statistical analysis cannot be used for data analysis). Subtraction of this relative OD cutoff from all relative ODs showed that residual relative OD values > 0.2 identified the presence of anti-ADAMTS13 antibodies against specific domains (Figure S3A-E), which is in accordance with the results obtained from statistical testing for the same patients (Figure 4A, E-F, K-L).

These results show that the library of 6 (AD1-M, AD1-DT, AD1-CS, AD1-T2-T5, AD1-T6-T8, AD1-CUB1-2) relatively small, nonoverlapping ADAMTS13 fragments enables fine mapping the anti-ADAMTS13 autoantibodies in patients with iTTP. Therefore, an epitope-mapping ELISA was established and validated and can now be used for the efficient and fast screening of samples from large cohorts of patients with iTTP.

4 | DISCUSSION

In this study, we generated a library of 6 small, nonoverlapping ADAMTS13 fragments that enable a more in-depth epitope mapping of anti-ADAMTS13 autoantibodies of patients with iTTP than previously described.⁵⁻⁷ Expression of these small fragments was realized

by using AD1 as an N-terminal fusion partner. The epitope-mapping ELISA using AD1-M, AD1-DT, AD1-CS, AD1-T2-T5, AD1-T6-T8, and AD1-CUB1-2 was set up and validated using the plasma of 18 patients with iTTP. With this, we developed a high-throughput method to fine map the anti-ADAMTS13 autoantibodies in large cohorts of patients with iTTP.

In-depth epitope mapping of anti-ADAMTS13 autoantibodies requires the availability of small ADAMTS13 fragments. Ideally, fragments corresponding to the 14 single domains of ADAMTS13 should be used. However, since previous work showed that expression of these single domains is not straightforward, we decided to express M, DT, C, S, T2-T5, T6-T8, CUB1, and CUB2. As an alternative option, we also expressed the MDT, MDTC, DTC, CS, T2-T8, and CUB1-2 fragments in case the individual domains M, C, S, CUB1, and CUB2, or small fragments like T2-T5 and T6-T8 would not be well expressed. In addition, we used the N-terminal fusion protein AD1 to enhance the secretion of all the fragments. This approach was successful as all fragments were expressed at relatively high levels. Studying the folding of all ADAMTS13 fragments using mouse or human anti-human ADAMTS13 monoclonal antibodies showed that the folding of only the single AD1-S and AD1-CUB1 was impaired. Of note, like all other ADAMTS13 fragments, the single domain ADAMTS13 fragments AD1-M and AD1-CUB2 were well folded. Hence, we succeeded in efficiently generating 6 small nonoverlapping ADAMTS13 fragments that covered the whole ADAMTS13 molecule (M, DT, CS, T2-T5, T6-T8, CUB1-2) for fine mapping of anti-ADAMTS13 autoantibodies, thereby avoiding the need to indirectly deduce the epitope of anti-ADAMTS13 autoantibodies.^{5,7} Additionally, all ADAMTS13 fragments are produced in mammalian cells, which, in contrast to bacterial³ and insect⁴ cells, enable posttranslational modifications similar to that observed in vivo.

The epitope mapping ELISA is simple (coating AD1-M, AD1-DT, AD1-CS, AD1-T2-T5, AD1-T6-T8 and AD1-CUB1-2; adding patient plasma and detection antibody) and only small plasma volumes (30 μ L) are needed, making the ELISA ideally suited for high-throughput epitope mapping of anti-ADAMTS13 autoantibodies. Moreover, only 1 repeat of the assay is sufficient to determine the antibody profile, by using the cutoff value determined by the negative control of AD1. As expected, in-depth immunoprofiling can be obtained only when the total anti-ADAMTS13 antibody titer or total anti-MDTC and anti-T2-C2 antibody titers are high enough. Low total anti-MDTC or anti-T2-C2 antibody titers will result in undetectable antibody binding when using the smaller fragments.

Since we analyzed only 18 plasmas of patients with iTTP for the validation of our assay, we cannot provide a meaningful discussion on the epitope mapping data we obtained in our study. We did notice that 4 of the 14 samples where we could determine the fine mapping did not contain detectable anti-CS antibodies. Since it has been reported that almost all patients with iTTP have anti-CS antibodies,³⁻⁷ we verified our data by screening these plasma samples on an ADAMTS13 variant where the ADAMTS13 spacer domain was swapped with an ADAMTS1 spacer domain. These data confirmed

that there are indeed no detectable anti-CS antibodies present in these plasma samples (unpublished data). Hence, these data support the good overall general folding of the AD1-CS fragment.

In conclusion, we generated an epitope-mapping ELISA based on 6 small, nonoverlapping ADAMTS13 fragments. This novel tool will allow a more in-depth epitope mapping than previously published⁵⁻⁷ and enables screening of large cohorts of patients with iTTP.

RELATIONSHIP DISCLOSURE

The authors declare no conflict of interest.

ACKNOWLEDGMENTS

This work was supported by the funding from the European Union's Horizon 2020 research and innovation program under the Marie Skłodowska-Curie grant agreement No 675746. The authors thank Airi Alajan, Tiiu Männik, and Kai Virumäe for their excellent technical assistance.

AUTHOR CONTRIBUTIONS

KK performed experiments, analyzed and interpreted the data, and wrote the manuscript. ER and SFDM interpreted data. ER, ASS, and JV provided the monoclonal antibodies. ET and GK provided plasma samples. AM designed the experiments and interpreted data. KV designed experiments, interpreted data, wrote the manuscript, and provided funding. All authors critically reviewed the manuscript.

TWITTER

Karen Vanhoorelbeke  @kvhoorel

REFERENCES

1. Kremer Hovinga JA, Coppo P, Lämmle B, Moake JL, Miyata T, Vanhoorelbeke K. Thrombotic thrombocytopenic purpura. *Nat Rev Dis Prim.* 2017;3:1-17.
2. Zheng X, Chung D, Takayama TK, Majerus EM, Sadler JE, Fujikawa K. Structure of von willebrand factor-cleaving protease (ADAMTS13), a metalloprotease involved in thrombotic thrombocytopenic purpura. *J Biol Chem.* 2001;276:41059-63.
3. Klaus C, Plaimauer B, Studt JD, Dorner F, Lämmle B, Mannucci PM, et al. Epitope mapping of ADAMTS13 autoantibodies in acquired thrombotic thrombocytopenic purpura. *Blood.* 2004;103:4514-9.
4. Luken BM, Turenhout EAM, Hulstein JJJ, Van Mourik JA, Fijnheer R, Voorberg J. The spacer domain of ADAMTS13 contains a major binding site for antibodies in patients with thrombotic thrombocytopenic purpura. *Thromb Haemost.* 2005;93:267-83.
5. Zheng XL, Wu HM, Shang D, Falls E, Skipwith CG, Cataland SR, et al. Multiple domains of ADAMTS13 are targeted by autoantibodies against ADAMTS13 in patients with acquired idiopathic thrombotic thrombocytopenic purpura. *Haematologica.* 2010;95:1555-62.
6. Pos W, Sorvillo N, Fijnheer R, Feys HB, Kaijen PHP, Vidarsson G, et al. Residues arg568 and phe592 contribute to an antigenic surface for anti-adamts13 antibodies in the spacer domain. *Haematologica.* 2011;96:1670-7.
7. Thomas MR, de Groot R, Scully MA, Crawley JTB. Pathogenicity of anti-ADAMTS13 autoantibodies in acquired thrombotic thrombocytopenic purpura. *EBioMedicine.* 2015;2:942-52.

8. Ostertag EM, Kacir S, Thiboutot M, Gulendran G, Zheng XL, Cines DB, et al. ADAMTS13 autoantibodies cloned from patients with acquired thrombotic thrombocytopenic purpura: 1. Structural and functional characterization in vitro. *Transfusion*. 2016;56:1763–74.
9. Lo K-M, Sudo Y, Chen J, Li Y, Lan Y, Kong S, et al. High level expression and secretion of Fc-X fusion proteins in mammalian cells. *Protein Eng*. 1998;11:495–500.
10. Feys HB, Liu F, Dong N, Pareyn I, Vauterin S, Vandeputte N, et al. ADAMTS-13 plasma level determination uncovers antigen absence in acquired thrombotic thrombocytopenic purpura and ethnic differences. *J Thromb Haemost*. 2006;4:955–62.
11. Plaimauer B, Kremer Hovinga JA, Juno C, Wolfsegger MJ, Skalicky S, Schmidt M, et al. Recombinant ADAMTS13 normalizes von Willebrand factor-cleaving activity in plasma of acquired TTP patients by overriding inhibitory antibodies. *J Thromb Haemost*. 2011;9:936–44.
12. Roose E, Schelpe A-S, Tellier E, Sinkovits G, Joly BS, Dekimpe C, et al. Open ADAMTS13, induced by antibodies, is a biomarker for subclinical immune-mediated thrombotic thrombocytopenic purpura. *Blood*. 2020;Apr 30:[Epub ahead of print].
13. Abroi A, Geimanen J, Janikson K, Mandel T, Silla T, Tagen I, et al. Vectors, cell lines and their use in obtaining extended episomal maintenance replication of hybrid plasmids and expression of gene products. Patent EP1851319B1. 2005.
14. Joung CH, Shin JY, Koo JK, Lim JJ, Wang JS, Lee SJ, et al. Production and characterization of long-acting recombinant human albumin-EPO fusion protein expressed in CHO cell. *Protein Expr Purif*. 2009;68:137–45.
15. Feys HB, Roodt J, Vandeputte N, Pareyn I, Lamprecht S, Van Rensburg WJ, et al. Thrombotic thrombocytopenic purpura directly linked with ADAMTS13 inhibition in the baboon (*Papio ursinus*). *Blood*. 2010;116:2005–10.
16. Deforche L, Roose E, Vandenbulcke A, Vandeputte N, Feys HB, Springer TA, et al. Linker regions and flexibility around the metalloprotease domain account for conformational activation of ADAMTS-13. *J Thromb Haemost*. 2015;13:2063–75.
17. Schelpe A, Petri A, Roose E, Pareyn I, Deckmyn H, De Meyer SF, et al. Antibodies that conformationally activate ADAMTS13 allosterically enhance metalloprotease domain function. *Blood Adv*. 2020;4:1072–80.
18. Roose E, Schelpe AS, Joly BS, Peetermans M, Verhamme P, Voorberg J, et al. An open conformation of ADAMTS-13 is a hallmark of acute acquired thrombotic thrombocytopenic purpura. *J Thromb Haemost*. 2018;16:378–88.
19. Feys HB, Vandeputte N, Palla R, Peyvandi F, Peerlinck K, Deckmyn H, et al. Inactivation of ADAMTS13 by plasmin as a potential cause of thrombotic thrombocytopenic purpura. *J Thromb Haemost*. 2010;8:2053–62.
20. Luken BM, Kaijen PHP, Turenhout EAM, Kremer Hovinga JA, Van Mourik JA, Fijnheer R, et al. Multiple B-cell clones producing antibodies directed to the spacer and disintegrin/thrombospondin type-1 repeat 1 (TSP1) of ADAMTS13 in a patient with acquired thrombotic thrombocytopenic purpura. *J Thromb Haemost*. 2006;4:2355–64.
21. Pos W, Luken BM, Kremer Hovinga JA, Turenhout EAM, Scheiflinger F, Dong JF, et al. VH1-69 germline encoded antibodies directed towards ADAMTS13 in patients with acquired thrombotic thrombocytopenic purpura. *J Thromb Haemost*. 2009;7:421–8.
22. Roose E, Vidarsson G, Kangro K, Verhagen OJHM, Mancini I, Desender L, et al. Anti-ADAMTS13 autoantibodies against cryptic epitopes in immune-mediated thrombotic thrombocytopenic purpura. *Thromb Haemost*. 2018;118:1729–42.
23. Karro K, Männik T, Männik A, Ustav M. DNA transfer into animal cells using stearylated CPP based transfection reagent. *Cell-Penetrating Pept Methods Protoc*. 2015;1324:435–45.
24. Moore A, Mercer J, Dutina G, Donahue CJ, Bauer KD, Mather JP, et al. Effects of temperature shift on cell cycle, apoptosis and nucleotide pools in CHO cell batch cultures. *Cytotechnology*. 1997;23:47–54.
25. Wong DCF, Wong KTK, Lee YY, Morin PN, Heng CK, Yap MGS. Transcriptional profiling of apoptotic pathways in batch and fed-batch CHO cell cultures. *Biotechnol Bioeng*. 2006;94:373–82.
26. Sorvillo N, Kaijen PH, Matsumoto M, Fujimura Y, van der Zwaan C, Verbij FC, et al. Identification of N-linked glycosylation and putative O-fucosylation, C-mannosylation sites in plasma derived ADAMTS13. *J Thromb Haemost*. 2014;12:670–9.
27. Verbij FC, Stokhuijzen E, Kaijen PHP, Van Alphen F, Meijer AB, Voorberg J. Identification of glycans on plasma-derived ADAMTS13. *Blood*. 2016;128:e51–e58.
28. Plaimauer B, Scheiflinger F. Expression and characterization of recombinant human ADAMTS-13. *Semin Hematol*. 2004;41:24–33.
29. Ricketts LM, Dlugosz M, Luther KB, Haltiwanger RS, Majerus EM. O-fucosylation is required for ADAMTS13 secretion. *J Biol Chem*. 2007;282:17014–23.
30. Zhou W, Tsai HM. N-Glycans of ADAMTS13 modulate its secretion and von Willebrand factor cleaving activity. *Blood*. 2009;113:929–35.

SUPPORTING INFORMATION

Additional supporting information may be found online in the Supporting Information section.

How to cite this article: Kangro K, Roose E, Schelpe A-S, et al. Generation and validation of small ADAMTS13 fragments for epitope mapping of anti-ADAMTS13 autoantibodies in immune-mediated thrombotic thrombocytopenic purpura. *Res Pract Thromb Haemost*. 2020;4:918–930. <https://doi.org/10.1002/rth2.12379>